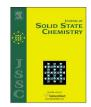


Contents lists available at ScienceDirect

### Journal of Solid State Chemistry



journal homepage: www.elsevier.com/locate/jssc

# A Ta/W mixed addenda heteropolyacid with excellent acid catalytic activity and proton-conducting property



Shujun Li<sup>a</sup>, Qingpo Peng<sup>a</sup>, Xuenian Chen<sup>a,\*</sup>, Ruoya Wang<sup>a</sup>, Jianxin Zhai<sup>a</sup>, Weihua Hu<sup>a</sup>, Fengji Ma<sup>b,\*</sup>, Jie Zhang<sup>a,\*</sup>, Shuxia Liu<sup>c</sup>

<sup>a</sup> School of Chemistry and Chemical Engineering, Henan Key Laboratory of Boron Chemistry and Advanced Energy Materials, Henan Normal University, Xinxiang, Henan 453007, China

<sup>b</sup> College of Chemistry and Chemical Engineering, Anyang Normal University, Anyang, Henan 453000, China

<sup>c</sup> Key Laboratory of Polyoxometalates Science of Ministry of Education, College of Chemistry, Northeast Normal University, Changchun City, Jilin 130024, PR China

#### ARTICLE INFO

Article history: Received 9 June 2016 Received in revised form 31 July 2016 Accepted 1 August 2016 Available online 2 August 2016

Keywords: Acid catalysis Heteropolyacid Ion-exchange Proton conduction Tantalum

#### 1. Introduction

Heteropolyacids (HPAs) constitute a small but important subclass in Polyoxometalates (POMs) family, which are usually acidic forms of typical POMs [1,2]. Their heteropolyanions (anion clusters usually made up of  $W^{VI}$  or  $Mo^{VI}$  and oxygen) have lower basicity on the surface oxygen atoms, so they are strong Brønsted acids and have significantly higher catalytic activity than mineral acids, such as sulfonic acid and hydrochloric acid. In particular in organic media, the molar catalytic activity of HPA is often 100–1000 times higher than that of  $H_2SO_4$ , and rarely leads to side reactions [3,4]. So, HPAs are highly suitable to catalyze various types of organic reactions in homogeneous liquid phase, and several processes with HPAs as the catalysts have been industrialized [1,5,6].

However, only limited HPAs with unambiguous structures determined by X-ray crystallography analysis or neutron diffraction analysis, including Keggin-type  $H_3[PW_{12}O_{40}] \cdot nH_2O$  [7–9], and  $H_3[PM_{012}O_{40}] \cdot nH_2O$  [10], Dawson-type  $H_7[In(H_2O)P_2W_{17}O_{61}] \cdot 23H_2O$  [11] and sandwich complex  $H_8[Ti_2\{P_2W_{15}O_{54}(OH_2)_2\}_2] \cdot 31H_2O$  [12], have been reported owing to the following two

#### ABSTRACT

A new HPAs  $H_{20}[P_8W_{60}Ta_{12}(H_2O)_4(OH)_8O_{236}] \cdot 125H_2O$  (H-1) which comprises a Ta/W mixed addenda heteropolyanion, 20 protons, and 125 crystalline water molecules has been prepared through ion-exchange method. The structure and properties of H-1 have been explored in detail. AC impedance measurements indicate that H-1 is a good solid state proton conducting material at room temperature with a conductivity value of  $7.2 \times 10^{-3}$  S cm<sup>-1</sup> (25 °C, 30% RH). Cyclic voltammograms of H-1 indicate the electrocatalytic activity towards the reduction of nitrite. Hammett acidity constant H<sub>0</sub> of H-1 in CH<sub>3</sub>CN is -2.91, which is the strongest among the present known HPAs. Relatively, H-1 exhibits excellent catalytic activities toward acetal reaction.

© 2016 Elsevier Inc. All rights reserved.

reasons. Firstly, most POMs compounds especially those with complex structures, are only stable under specific narrow pH ranges, and tend to convert into stable Keggin or Dawson species under strong acid conditions. Secondly, it is difficult to obtain single crystals of some HPAs suitable for X-ray diffraction measurements. Exploring novel type HPAs other than traditional Keggin or Dawson type is motivating for the farther development of HPAs and relevant acid catalysis areas.

On the other hand, although POMs based on  $V^V$ ,  $Mo^{VI}$ ,  $W^{VI}$ , and now even Nb<sup>V</sup> provide frequent exciting advances, little is known about the POM chemistry of Ta<sup>V</sup> [13]. The first polyoxotantalate (K<sub>8</sub>[Ta<sub>6</sub>O<sub>19</sub>]) was discovered more than sixty years ago, but the synthesis of Ta-containing POMs is still challenging, mainly because the soluble Ta precursors (e.g.  $[Ta_6O_{19}]^{8-}$  or  $TaCl_5$ ) tend to form intractable gel-like materials or Ta<sub>2</sub>O<sub>5</sub> precipitate in aqueous solution [14,15]. Recently our group and Nyman's group have demonstrated that it is feasible to access mixed metal Ta/W POMs in acidic solution [16,17]. These Ta/W mixed addenda POMs will provide excellent opportunity for the further development of Ta-POMs chemistry, because they exhibit unique property compared with the related Ta-POMs and W-POMs in term of electronic and electrochemical properties, solubility, stability, reactivity and photocatalytic performance. However, the research is still at the early stage, and only few examples of Ta/W mixed addenda compounds are known so far [18]. Much systematic and extended work still needs to do in this field.

<sup>\*</sup> Corresponding author. *E-mail addresses:* xnchen@htu.edu.cn (X. Chen), fengji.ma@yahoo.com (F. Ma), jie.zhang@htu.edu.cn (J. Zhang).

It has been demonstrated that Ta/W mixed addenda monomers have strong tendency to form aggregates by the formation of steady Ta–O–Ta bridges in acidic solution [17]. The very good stability of the polymerized Ta/W POMs in strong acid solution makes them promising for a new type of HPAs. In this report a full-acid (free-acid) form of tetrameric Ta/W mixed addenda POM  $H_{20}[P_8W_{60}Ta_{12}(H_2O)_4(OH)_8O_{236}] \cdot 125H_2O$  (H-1) has been isolated as yellow crystals through ion-exchange method. The structure and properties of H-1 have been discussed in detail. The acidity has been measured by UV–Vis spectrophotometry using a Hammett indicator. H-1 exhibits excellent homogeneous acid catalytic activity and proton-conducting ability in solid state.

#### 2. Experimental section

#### 2.1. Materials and measurement

The precursor  $K_8Na_8H_4[P_8W_{60}Ta_{12}(H_2O)_4(OH)_8O_{236}] \cdot 42H_2O(1)$ was synthesized according to the procedure described in the literature [17]. All other reagents were readily available from commercial sources and used without further purification. The FTIR spectra in KBr pellets were recorded in the range 400–4000 cm<sup>-1</sup> with a VECTOR 22 Bruker spectrophotometer at room temperature. Elemental analyses for P, W, and Ta were determined with a PLASMASPEC (I) ICP atomic emission spectrometer. Powder X-ray diffraction (PXRD) measurements were performed on a Bruker D8 Advance Instrument with Cu K $\alpha$  radiation in the angular range  $2\theta = 3-50^{\circ}$  at 293 K. The thermal behavior of **H-1** was examined by synchronousthermal analyses (TG/DSC, Netzsch 449 C Jupiter/QMS 403D). The samples were heated to 700 °C with a heating rate of  $5 \circ C$  /min, under a flowing N<sub>2</sub> atmosphere. UV–Vis absorption spectra were obtained by using a UV-1700 UV-Vis spectrophotometer. The <sup>31</sup>P NMR spectra were measured on Avance-400 Bruker NMR spectrometers at an operating frequency of 16.66 MHz, with a 2.5 kHz sweep width, and 5-s pulse delay. Electrochemical measurements were performed with CHI1604E electrochemical workstation (Chenhua Instruments Co., Shanghai, China). Three-electrode system was employed in this study, a glass carbon electrode used as the working electrode, a Ag/AgCl electrode used as the reference electrode and a Pt coil used as the counter electrode. All the experiments were conducted at ambient temperature (20-25 °C).

#### 2.2. Crystal structure determination

Single crystal XRD analysis of **H-1** was conducted on a Bruker Smart Apex CCD diffractrometer with Mo K $\alpha$  monochromated radiation ( $\lambda$ =0.71073 Å) at room temperature. The linear absorption coefficients, scattering factors for the atoms, and anomalous dispersion corrections were taken from the International Tables for X-Ray Crystallography [19]. Empirical absorption corrections were applied. The structures were solved by using the direct method and refined through the full matrix least-squares method on F<sup>2</sup> using SHELXS-97 [20]. Anisotropic thermal parameters were used to refine all nonhydrogen atoms. Those hydrogen atoms attached to lattice water molecules were not located. The crystal data and structure refinement results of H-1 are summarized in Table 1. Further details on the crystal structure investigation scan be obtained free of charge from The Cambridge Crystallographic Data Centre via www.ccdc.cam.ac. uk/data\_request/cif (depository number CCDC-1457311).

#### 2.3. Proton conductivity measurement of H-1

Ac impedance spectroscopy measurement was performed on a chi660d (Shanghai chenhua) electrochemical impedance analyzer

[able ]	1
---------	---

Crystal data and structural refinement for compound H-1.

Compound	H-1
Formula	$H_{20}[P_8W_{60}Ta_{12}(H_2O)_4(OH)_8O_{236}] \cdot 125H_2O$
Formula weight (gmol <sup>-1</sup> )	18,729.56
T (K)	103 (2)
Wavelength (Å)	0.71073
Crystal system	Tetragonal
Space group	P-421c
a (Å)	24.185(2)
b (Å)	24.185(2)
<i>c</i> (Å)	27.067(3)
α (°)	90
β(°)	90
γ (°)	90
<i>V</i> (Å <sup>3</sup> )	15,832(3)
Ζ	2
$D_{calc} (\text{mg m}^{-3})$	3.929
$\mu(\mathrm{mm}^{-1})$	25.978
F(000)	16,152.0
Crystal dimensions mm <sup>-1</sup>	$0.30 \times 0.26 \times 0.20$
Goodness-of-fit on $F^2$	0.907
Final <i>R</i> indices[ $I > 2\sigma(I)$ ]	$R_1^a = 0.0855$ , $wR_2^a = 0.1581$
R indices (all data)	$R_1^{a} = 0.1585, wR_2^{a} = 0.1942$

<sup>a</sup>  $R_1 = \sum ||F_0| - |F_c|| / \sum |F_0|$ ;  $wR_2 = \{\sum [w(F_0^2 - F_c^2)^2] / \sum [w(F_0^2)^2] \}^{1/2}$ .

with copper electrodes (the purity of Cu is more than 99.8%) over the frequency range from 105 to 1 Hz. The powdered crystalline sample of **H-1** was compressed to 1.0–1.2 mm in thickness and 12.0 mm in diameter under a pressure of 12–14 MPa at room temperature. The conductivities were determined from the Nyquist plots. According to the Nyquist plot for H-1 at each temperature and humidity, the proton conductivity was calculated as  $\sigma = (1/R) (h/S)$ , where *R* is the resistance, *h* is the thickness, and *S* is the area of the disk. The activation energy was calculated from the Arrhenius plot according to the formula  $\sigma T = \sigma_0 \exp(-Ea/k_BT)$ . Real (*Z*') and imaginary (*Z*") parts of the impedance spectra are shown in Fig. 6 and Figs. S9–S10.

#### 2.4. Acid strength measurement of H-1

Acidity measurements of **H-1** were performed in acetonitrile according to the procedure described in the literatures [21,22]. Dicinnamylideneacetone (p*K*a value is -3.0, where *Ka* is the dissociation constant of the protonated indicator p*K*a =  $-\log Ka$ ) was used as indicator. The concentration of Dicinnamylideneacetone and proton (based on the number of protons per HPAs) were set to  $7 \times 10^{-4}$  mol/L and  $9.72 \times 10^{-4}$  mol/L respectively. UV–vis absorption spectra were obtained by using a UV-1700 UV–Vis spectrophotometer. The Hammett acidity function ( $H_0$ ) is defined by  $H_0 = pKa - \log[BH^+]/[B]$ . [BH<sup>+</sup>] and [B] are the concentrations of the protonated and neutral forms of the indicator in the equilibrium  $BH^+ \Rightarrow B + H^+$ . The ratio of the extinction coefficient of the two forms was estimated to be 1.3 by  $H_3PW_{12}O_{40}$  (Fig. S11 and S12).

#### 2.5. Preparation of $H_{20}[P_8W_{60}Ta_{12}(H_2O)_4(OH)_8O_{236}] \cdot 125H_2O$ (H-1)

400 mL 1 M HCl solution was poured into a column with an inner diameter of 15 mm charged with 100 g cationic exchange resin (Amberlite IR120B NA). A dripping rate of one drop/2 s was used. After that, the column was washed with deionized water to neutral.

3.0 g precursor (1) was dissolved in 5.0 mL deionized water, the resulting clear solution was passed through the above mentioned cation-exchange resin column at a dripping rate of one drop/2 s, then washed with deionized water to neutral. The collected solution was evaporated on a rotary evaporator at 80 °C, resulting in a

Download English Version:

## https://daneshyari.com/en/article/1329389

Download Persian Version:

https://daneshyari.com/article/1329389

Daneshyari.com